THE JOURNAL OF BIOLOGICAL CHEMISTRY
Vol. 280, No. 9, Issue of March 4, pp. 7659–7670, 2005
Printed in U.S.A.

Role of the Degree of Oligomerization in the Structure and Function of Human Surfactant Protein A*

Received for publication, September 7, 2004, and in revised form, December 16, 2004
Published, JBC Papers in Press, December 21, 2004, DOI 10.1074/jbc.M410266200

Fernando Sánchez-Barbero‡§, Jochen Strassner¶‖, Rafael García-Cañero, Wolfram Steinhilber¶, and Cristina Casals‡ ‡‡**

*From the ‡Department of Biochemistry and Molecular Biology I, Complutense University of Madrid, 28040 Madrid, Spain, the **Department of Experimental Biochemistry, Hospital Puerta de Hierro, 28035 Madrid, Spain, and the ¶Department of Biotechnology, ALTANA Pharma AG, Byk-Gulden-Strasse 2, 78467 Konstanz, Germany*

The role of the degree of oligomerization in the structure and function of human surfactant protein A (SP-A) was investigated using a human SP-A1 mutant (SP-A1$^{\Delta AVC,C6S}$), expressed in mammalian cells, resulting from site-directed substitution of serine for Cys^6 and substitution of a functional signal peptide for the cysteine-containing SP-A signal sequence. This Cys^6 mutant lacked the NH_2-terminal Ala^{-3}-Val^{-2}-Cys^{-1} (ΔAVC) extension present in some SP-A1 isoforms. SP-A1$^{\Delta AVC,C6S}$ was assembled exclusively as trimers as detected by electron microscopy and size exclusion chromatography. Trimeric SP-A1$^{\Delta AVC,C6S}$ was compared with supratrimeric SP-A1, which is structurally and functionally comparable to the octadecameric protein isolated from human lung lavages. SP-A1$^{\Delta AVC,C6S}$ showed reduced thermal stability of the collagen domain, studied by circular dichroism, and increased susceptibility to trypsin degradation. The T_m was 32.7 °C for SP-A1$^{\Delta AVC,C6S}$ and 44.5 °C for SP-A1. Although SP-A1$^{\Delta AVC,C6S}$ was capable of binding to calcium, rough lipopolysaccharide, and phospholipid vesicles, this mutant was unable to induce rough lipopolysaccharide and phospholipid vesicle aggregation, to enhance the interfacial adsorption of SP-B/SP-C-surfactant membranes, and to undergo self-association in the presence of Ca^{2+}. On the other hand, the lack of supratrimeric assembly hardly affected the ability of SP-A1$^{\Delta AVC,C6S}$ to inhibit the production of tumor necrosis factor-α by macrophage-like U937 cells stimulated with either smooth or rough lipopolysaccharide. We conclude that supratrimeric assembly of human SP-A is essential for collagen triple helix stability at physiological temperatures, protection against proteases, protein self-association, and SP-A-induced ligand aggregation. The supratrimeric assembly is not essential for the binding of SP-A to ligands and anti-inflammatory effects of SP-A.

Surfactant protein A (SP-A)[1] is a large oligomeric extracellular protein primarily found in the alveolar fluid of mammals. SP-A is a lipid-binding protein, a property that allows it to position and concentrate along with the extracellular membranes that line the alveolar epithelium and constitute the pulmonary surfactant. Thus, surfactant membranes containing SP-B and SP-C are bedecked with SP-A, which interacts primarily at bilayer surfaces. In relation to the surfactant system, SP-A catalyzes the formation of tubular myelin, improves the adsorption and spreading of surfactant membranes onto an air-liquid interface, and protects surfactant biophysical activity from the inhibitory action of serum proteins (1–3). At the same time, this tight binding of SP-A to surfactant membranes makes possible its strategic location at the front lines of defense against inhaled pathogens, toxins, and allergens. SP-A recognizes pathogen-associated molecular patterns on microorganisms, resulting in aggregation, opsonization, or permeabilization of microorganisms and facilitation of microbial clearance (1, 4–7). Moreover, SP-A is capable of direct interaction with epithelial and immune cells in the alveolus through binding to cell membrane receptors. This results in modulation of immune cell functions such as phagocytosis of pathogens and apoptotic cells, chemotaxis, proliferation, cytokine production, respiratory burst, and expression of surface receptors (1, 6–9). Thus, SP-A is involved in innate host-defense and inflammatory immunomodulator processes of the lung, as demonstrated by experiments with mice deficient in SP-A. These SP-A knockout mice show increased susceptibility to bacterial and viral infections (10) and enhanced inflammatory responses in the lung to a variety of stimuli (11).

The binding capabilities of SP-A to surfactant membranes, pathogen-associated molecular patterns, and receptors on cell surfaces depend on its complex structure. SP-A belongs to the structurally homologous family of innate immune defense proteins known as collectins for their collagen-like and lectin domains. The primary structure of mature SP-A is conserved among different mammals with some differences. It consists of four structural domains: 1) an NH_2-terminal segment involved in intermolecular disulfide bond formation; 2) a collagen-like

* This work was supported in part by QLK2-CT-2000-00325 from the European Community and FIS 03/0137. We acknowledge the support of Centro de Asistencia a la Investigación de Espectroscopía of Universidad Complutense de Madrid. The costs of publication of this article were defrayed in part by the payment of page charges. This article must therefore be hereby marked "*advertisement*" in accordance with 18 U.S.C. Section 1734 solely to indicate this fact.

§ Recipient of a grant from Ministerio de Educación y Ciencia (Grant FPU-AP2002-0301).

‖ Supported by the European Community Grant QLK2-CT-2000-00325.

‡‡ To whom correspondence should be addressed: Dept. of Biochemistry and Molecular Biology I, Faculty of Biology, Complutense University of Madrid, 28040 Madrid, Spain. Tel.: 34-91-394-4261; Fax: 34-91-394-4672; E-mail: ccasalsc@bio.ucm.es.

[1] The abbreviations used are: SP-A, surfactant protein A; CD, circular dichroism; CHO, Chinese hamster ovary; dansyl-DHPE, dansyl-1,2-hexadecanoyl-*sn*-glycero-3-phosphoethanolamine; DPPC, 1,2-dipalmitoyl-*sn*-glycero-3-phosphocholine; DPPG, 1,2-dipalmitoyl-*sn*-glycero-3-phosphoglycerol; FBS, heat-inactivated fetal bovine serum; FRET, fluorescence resonance energy transfer; FITC, fluorescein-5-isothiocyanate; LES, lipid extract from surfactant; Re-LPS, rough lipopolysaccharide; s-LPS, smooth lipopolysaccharide; SP-D, surfactant protein D; SP-A1$^{\Delta AVC,C6S}$, Cys^{-1}- and Cys^6-deficient mutant SP-A1 expressed in CHO cells; PHA, phytohemagglutinin; T_m, midpoint transition melting temperature; TNF, tumor necrosis factor.

domain characterized by 23 Gly-*X*-*Y* repeats with an interruption near the midpoint of the domain; 3) an α-helical coiled-coil domain, which constitutes the neck region between the collagen and the globular domain; and 4) a COOH-terminal globular domain involved in phospholipid binding and in Ca^{2+}-dependent binding of oligosaccharides (12, 13). SP-A is modified after translation (cleavage of the signal peptide, proline hydroxylation, and Asn^{187}-linked glycosylation). Unlike SP-As from other mammalian species, baboon and human SP-As consist of two polypeptide chains, SP-A1 and SP-A2. The major differences between mature SP-A1 and SP-A2 are in the collagen domain (14).

The oligomerization domains in SP-A and other collectins are the coiled-coil domain, collagen triple helices, and the NH_2-terminal segment. SP-A oligomerization is an intracellular process that is thought to occur in a zipper-like fashion along the C-terminal to N-terminal axis, as reported for other collectins (SP-D and MBL-C) (15, 16). Triple-helix formation from three polypeptide chains requires previous trimerization of COOH-terminal globular domains by a trimeric α-helical coiled-coil (13, 17, 18). Octadecamers appear to be formed by lateral association of the NH_2-terminal half of six triple-helical stems, forming a microfibrillar end piece stabilized by disulfide bonds at the NH_2-terminal region (19, 20) (see Fig. 1). In rat SP-A two cysteine residues are involved in multimer formation: a cysteine in the 6 position of the NH_2-terminal segment (17) and another cysteine in the position −1, which is the last position of the signal peptide, one amino acid before the NH_2 terminus (18). Human SP-A, as well as recombinant human SP-A1 and SP-A2, expressed in mammalian or insect cells, also has considerable NH_2-terminal heterogeneity, in which about 50–75% of human SP-A molecules contain Cys^{-1} isoforms (18, 21–23). In human SP-A1, four cysteine residues are potentially involved in the arrangement of the disulfide bonding: two cysteine residues in the NH_2-terminal segment (Cys^{-1} and Cys^6), another in the middle of the collagen-like sequence within the Pro-Cys-Pro-Pro interruption (Cys^{48}), and a fourth cysteine at position 65 (Cys^{65}) in the collagen domain near the neck. Cys^{65} is substituted by Arg^{65} in the human SP-A2 polypeptide chain (14).

The first objective of this study was the production of a full-length mammalian cell-derived SP-A1 molecule that was not capable of forming higher oligomers than trimers. To this end, the cysteine at position +6 was removed by site-direct mutagenesis (Ser was substituted for Cys^6). In addition, human IgG light-chain signal sequence was substituted for SP-A1 signal sequence to abolish the Cys^{-1} isoforms. The combined mutation eliminates potential inter-chain disulfide cross-linking within the NH_2-terminal portion of the molecule. Using this approach, we produced a full-length mutant SP-A molecule ($SP\text{-}A1^{\Delta AVC,C6S}$) that is secreted as a trimer, utilizing a CHO K1 cell expression system. The second objective was the analysis of the structure and function of $SP\text{-}A1^{\Delta AVC,C6S}$ in comparison with wild type recombinant human SP-A1, expressed in the same system, which has a supratrimeric assembly and is functionally comparable to the protein isolated from lung lavages of healthy subjects (22).

Although several studies have indicated the importance of the degree of oligomerization in mannose-binding protein and mammalian cell-derived SP-D (24–26), none have dealt with the functional importance of supratrimeric assembly in SP-A expressed in mammalian cells. These results are important in understanding the consequences of incomplete oligomerization, because the extent of oligomerization of human SP-A may be altered in various disease states and can vary among individuals (27). Incomplete oligomerization occurs in insect cell-derived human SP-A1, which consists mainly of trimers and hexamers and low levels of higher oligomers (22, 23). Insect cells lack prolyl 4-hydroxylase activity. The lack of hydroxyproline perturbs the folding of recombinant human SP-A1, which influences the arrangement of disulfide bonding, affecting the oligomerization of nascent hydroxyproline-deficient SP-A1 (22).

In this study we report for the first time that the supratrimeric assembly is essential for the stabilization of the collagen triple helix of mammalian cell-derived human SP-A1 at physiological temperatures. The collagen triple helix of $SP\text{-}A1^{\Delta AVC,C6S}$ is partially unfolded at 37 °C, which increases the susceptibility of the protein to proteolytic degradation. In addition, our results show that supratrimeric assembly of human SP-A1 is essential for 1) Ca^{2+}-dependent SP-A self-association, 2) the capability of SP-A to induce aggregation of membranes and LPS micelles, and 3) the ability of SP-A to enhance surfactant interfacial adsorption. However, supratrimeric assembly is not essential for the binding of human SP-A to phospholipids and rough-LPS and for the anti-inflammatory activity of SP-A.

EXPERIMENTAL PROCEDURES

Materials—Synthetic phospholipids, DPPC and DPPG, were purchased from Avanti Polar Lipids (Birmingham, AL), and their homogeneity was routinely tested on thin-layer chromatography. Dansyl-DHPE, fluorescein, and fluorescenin-5-isothiocyanate (FITC, isomer I) were obtained from Molecular Probes (Eugene, OR). Rough LPS from *Salmonella minnesota* (serotype Re-595), smooth LPS from *Escherichia coli* (serotype 055:B5), FITC-LPS from *E. coli* (serotype 055:B5), trypsin from bovine pancreas, phorbol 12-myristate 13-acetate, and PHA were purchased from Sigma Co. The organic solvents (methanol and chloroform) used to dissolve lipids were high-performance liquid chromatography grade (Scharlau, Barcelona). RPMI 1640 medium, heat-inactivated fetal bovine serum, and a *Limulus* amebocyte lysate kit were obtained from Bio-Whittaker (Walkersville, MD). Gradient SDS-PAGE gels were from NOVEX (Invitrogen). An enzyme-linked immunosorbent assay kit for TNF-α immunoassays was obtained from BD Pharmingen (San Diego, CA). Macrophage-like cell line U937 cells were supplied by the American Type Culture Collection (Manassas, VA). Anti-CD14 (28C5) was kindly provided by Dr. Peter Tobias (The Scripps Research Inst., La Jolla, CA). All other reagents were of analytical grade obtained from Merck.

Expression and Purification of Recombinant Human SP-A1—The recombinant wild-type form of human SP-A1 ($6A^2$ allele) was expressed in stably transformed CHO K1 cells as described by Voss *et al.* (19) and purified from culture supernatant by mannose affinity chromatography. Endotoxin content was 200 pg/mg of SP-A1 as determined by *Limulus* amebocyte lysate assay.

Cloning and Expression of Recombinant Human $SP\text{-}A1^{\Delta AVC,C6S}$ Mutant—The genomic DNA sequence of the human SP-A1 gene contained in the expression vector as described in Voss *et al.* (19), was subcloned into the expression vector pEFmyc/cyto (Invitrogen) in which the myc epitope was removed after digestion with NotI/XbaI. Furthermore, the signal sequence of SP-A1 was replaced by the signal sequence Vκ21G of the light chain of a human IgG. The expression plasmid was introduced into CHO K1 cells by polyfectamine (Invitrogen) as transfection reagent using standard conditions. Stably expressing cell clones were selected in 1 mg/ml G418 and subsequently subcloned by limited dilution. For expression, the cells were grown in roller bottles using serum-free Dulbecco's modified Eagle's medium/Ham's F-12 supplemented with 10 mM Hepes and 1 mM ascorbate for hydroxylation as described previously (19).

Purification of Recombinant Human $SP\text{-}A1^{\Delta AVC,C6S}$ Mutant—Given that $SP\text{-}A1^{\Delta AVC,C6S}$ trimers are poorly isolated by mannose affinity chromatography, we have developed a new method of SP-A isolation. $SP\text{-}A1^{\Delta AVC,C6S}$ trimers were purified from culture supernatant by anionic exchange chromatography, size exclusion chromatography, and hydrophobic interaction chromatography.

All chromatography steps were carried out at room temperature on an extended Äkta Purifier chromatography system (Amersham Biosciences), using sterile buffers. Typically, 5 liters of cell culture supernatant were centrifuged at 11,000 × *g* for 1 h, at 4 °C in a Sorvall Evolution RC centrifuge using a SLC-6000 rotor (Kendro Laboratory Products). The resulting supernatant was diluted with one volume of

anionic exchange chromatography buffer A (20 mM borate, pH 10) to decrease conductivity, and subsequently sterilized by filtration (ZapCap Plus, 0.2 μm, Schleicher & Schuell, Dassel, Germany). The resulting 10-liter sample was then passed through a 50-ml Resource Q anion exchanger column (Amersham Biosciences) at 478 ml/h. Bound protein was eluted with a salt gradient elution, ranging from 0 to 45% anionic exchange chromatography buffer B (20 mM borate, pH 10, 1 M NaCl) at 190 ml/h flow rate. Fractions containing SP-A1$^{\Delta AVC,C6S}$ were pooled, concentrated, and buffered into size exclusion chromatography running buffer (25 mM Tris/HCl, pH 7.5, 0.15 M NaCl; 2 mM EDTA; 0,02% NaN_3) using an Amicon stirring chamber (Millipore, Schwalbach, Germany) with a 30-kDa cutoff nitrocellulose membrane. Two milliliters of the sample were then applied to a 300-ml Superdex 200 column (Amersham Biosciences) at a flow rate of 28 ml/h. Fractions eluting at an apparent molecular mass of 105 kDa contained SP-A1$^{\Delta AVC,C6S}$. These fractions were pooled, concentrated, and buffered into hydrophobic interaction chromatography buffer A (25 mM Tris/HCl, pH 7.5, 0.8 M $(NH_4)_2SO_4$). After sterile filtration, a volume of 14 ml was applied to a 20-ml Phenyl-Sepharose HP column (Amersham Biosciences) at 90 ml/h, and SP-A1$^{\Delta AVC,C6S}$ was eluted with a salt gradient elution, from 0 to 100% hydrophobic interaction chromatography buffer B (25 mM Tris/HCl, pH 7.5). Subsequently, the buffer was exchanged for 10 mM $NaHPO_4$, pH 7.5, and the protein concentration was adjusted to 2 mg/ml. The endotoxin content was <0.5 enzyme units/mg SP-A (50 pg/mg SP-A) as determined by the *Limulus* amebocyte lysate assay. The purity of the final product was >95% according to the quantification using the Agilent Bioanalyzer 2100 system and the Protein 200 plus LabChip Kit (Agilent Technologies, Waldbronn, Germany). The suitability of this new method of SP-A isolation was checked with human SP-A from alveolar proteinosis. Human SP-A isolated by this new method exhibited structural and functional properties similar to the protein isolated by butanol and octylglucoside extractions (28), but the endotoxin content was much lower.[2]

Isolation of Human SP-A—Bronchoalveolar lavages from alveolar proteinosis patients were used as a source of human SP-A. SP-A was purified from isolated surfactant using sequential butanol and octylglucoside extractions (28) Endotoxin content of natural human SP-A isolated by this method was about 300 pg of endotoxin/mg of SP-A, as determined by *Limulus* amebocyte lysate test. Quantification of SP-A was carried out by amino acid analysis in a Beckman System 6300 High Performance analyzer as described elsewhere (29).

Protein Microsequencing—The NH_2-terminal amino acid sequence of SP-A1 and SP-A1$^{\Delta AVC,C6S}$ was determined using a modification of the technique of Edman degradation on an automated gas phase microsequencer (ABI Protein sequencer) as described previously (30). Proteins were submitted for analysis bound to polyvinylidene difluoride membranes after transfer from SDS-PAGE. The relative percentage of the SP-A isoforms was estimated by comparison of the molecular yield of representative amino acids from each sequence.

Polyacrylamide Gel Electrophoresis—Purity and apparent molecular weights of monomeric SP-As were determined by 12% SDS-PAGE under reducing conditions (5% β-mercaptoethanol). Proteins were visualized by silver stain (22). Pre-stained See Blue (NOVEX) was used as molecular weight marker.

To determine the assembly of disulfide-linked polypeptide chains of SP-A samples, 50 ng of each of the SP-As was separated on a precasted 4–12% gradient SDS-PAGE under non-reducing conditions. The SP-A proteins were detected by Western blotting using anti-human SP-A anti-serum raised in rabbits in a dilution of 1:100,000 and were visualized by chemiluminescence. The molecular weight of the disulfide-linked oligomers was determined by comparison with a molecular weight standard. For native conditions, electrophoresis was performed at 4 °C with a 7% Tris acetate polyacrylamide gel (NOVEX) in the absence of reducing agents as described previously (22).

Electron Microscopy—The sample preparation for electron microscopy was carried out as described in a previous study (19). 25 ng of SP-A1 and SP-A1$^{\Delta AVC,C6S}$ was dissolved in 0.2 M ammonium bicarbonate, pH 7.9, mixed with an equal volume of glycerol, and immediately sprayed onto freshly cleaved mica. Rotary shadowing by platinum/carbon and electron microscopy was done following protocols described previously (31).

CD Measurements—CD spectra were obtained on a Jasco J-715 spectropolarimeter fitted with a 150-watt xenon lamp (22, 23, 32). Quartz cells with a 1-mm path length were used, and the spectra were recorded in the far-UV region (190–260 nm) at the indicated temperature. Four scans were accumulated and averaged for each spectrum. The acquired spectra were corrected by subtracting the appropriate blanks, subjected to noise-reduction analysis, and presented as molar ellipticities (degrees·cm^2·dmol^{-1}) assuming 110 Da as the average molecular mass per amino acid residue. All measurements were typically performed in 5 mM Tris-HCl buffer, pH 7.4, in the absence or presence of 1 mM calcium and 150 mM NaCl. Protein concentration in all cases was 120 μg/ml and was determined by amino acid analysis.

For the analysis of thermal stability of the collagen-like domain of recombinant human SP-As, melting curves were monitored at 207 nm while the sample temperature was raised from 10 to 70 °C, with an average heating rate of 12 °C/h. SP-A concentrations were 120 μg/ml, and quartz cells with a 1-mm path length were used. The folded fraction was calculated from the equation: $F = ([\theta] - [\theta]_u)/([\theta]_n - [\theta]_u)$, where $[\theta]$ is the observed mean residue molar ellipticity at 207 nm, and $[\theta]_n$ and $[\theta]_u$ are the mean values for natural and unfolded SP-A, respectively. These values were obtained from the plateau before and after the transition. The temperature where the collagen triple helix of SP-A was 50% unfolded ($F = 0.5$) was taken as the melting temperature (T_m).

Trypsin Digestion—To determine the protease sensitivity of SP-A1 and SP-A1$^{\Delta AVC,C6S}$ at temperatures above and below the T_m of the corresponding protein, the recombinant proteins (2 μg) were incubated with trypsin (0.13 μg) in 5 mM Tris-HCl buffer (pH 7.4) as described before (32, 33). The mixtures were incubated during 30 min at 25, 37, and 50 °C. The digestion was stopped by addition of reducing SDS-PAGE sample buffer containing phenylmethylsulfonyl fluoride followed by boiling. Samples were analyzed by SDS-PAGE followed by silver stain. To test the effect of the binding of Ca^{2+} to SP-A on trypsin susceptibility, SP-A1 and SP-A1$^{\Delta AVC,C6S}$ were incubated in a 5 mM Tris-HCl buffer (pH 7.4) containing 100 mM NaCl, and 1 mM $CaCl_2$ for 10 min prior to 30-min incubation with trypsin at the indicated temperatures.

Intrinsic Fluorescence—Fluorescence measurements were carried out using an SLM-Aminco AB-2 spectrofluorometer with a thermostatted cuvette holder (±0.1 °C), using 5 × 5 mm path-length quartz cuvettes. Fluorescence emission spectra of human SP-A (7 μg/ml) were measured at 25 °C in 5 mM Tris-HCl buffer (pH 7.4) containing either 2 mM Ca^{2+} or 2 mM EDTA (22, 23, 29). The blanks and protein samples were excited at 275 nm for measuring the total protein fluorescence spectrum. The slit widths were 4 nm for the excitation and emission beams. Emission spectra were recorded from 300 to 400 nm.

Fluorescence Assays to Determine the Binding of SP-A to FITC-Re-LPS—A fluorescent Re-LPS derivative (FITC-Re-LPS) in which the phosphoethanolamine groups of Re-LPS were bound to fluorescein isothiocyanate (FITC) was prepared by the method described before (34). The Re-LPS concentration of the fluorescent derivative was determined by quantification of the 2-keto-3-deoxyoctulosonic acid, and the content of fluorescein was determined by optical density at 493 nm as described (34). Typically, the fluorescent Re-LPS derivative had substitution ratios of 15–20 mol% fluorescein. Fluorescence emission spectra of FITC-Re-LPS (1 μg/ml) were measured in the presence and absence of SP-A (50 μg/ml) in 150 mM NaCl, 1 mM EDTA, 5 mM Tris-HCl buffer (pH 8) at 25 °C. The blanks (protein alone) and FITC-Re-LPS samples (with and without protein) were excited at 470 nm, and emission spectra were recorded from 500 to 650 nm. Fluorescence emission anisotropy measurements were obtained with Glan Prism polarizers. Excitation and emission wavelengths were set at 470 and 520 nm, respectively. For each sample, fluorescence emission intensity data in parallel and perpendicular orientations with respect to the exciting beam were collected ten times each and then averaged. Anisotropy, r, was calculated as,

$$r = \frac{I_{\parallel} - GI_{\perp}}{I_{\parallel} + 2GI_{\perp}} \quad \text{(Eq. 1)}$$

where $I_{\parallel}$ and $I_{\perp}$ are the parallel and perpendicular polarized intensities measured with the vertically polarized excitation light, and G is the monochromator grating correction factor.

Fluorescence Resonance Energy Transfer Assay to Determine the Binding of SP-A to Phospholipid Vesicles—DPPC vesicles containing different mol % of dansyl-DHPE (from 0–5 mol%) were prepared at the indicated phospholipid concentrations (5, 10, 20, 40, or 60 μg/ml) by hydrating dry lipid films in buffer A containing 100 mM NaCl, 0.1 mM EDTA, 5 mM Tris-HCl (pH 7.4) and allowing them to swell for 1 h at 51 °C. After vortexing, the resulting multilamellar vesicles were sonicated at the same temperature during 2 min at 390 watts/cm^2 (burst of 0.6 s, 0.4 s between bursts) in a UP 200S sonifier with a 2-mm microtip. Unilamellar vesicles were prepared freshly each day, just before start-

[2] F. H. Bosch, F. Sánchez-Barbero, W. Steinhilber, and C. Casals, unpublished results.

ing the experiment. The final lipid concentration was assessed by phosphorus determination. For vesicle-size analysis in solution, quasi-elastic light scattering was used as recently described (35). DPPC vesicles prepared by sonication consisted of a major population (70%) of unilamellar vesicles (mean diameter of 105 ± 6 nm) and a minor population (30%) of multilamellar vesicles (mean diameter of ~2 μm) that were removed by centrifugation. The maximum excitation and emission wavelengths of dansyl-DHPE/DPPC vesicles in buffer A were 340 and 523 nm, respectively.

Fluorescence resonance energy transfer (FRET) from SP-A tryptophan residues to the dansyl extrinsic probe incorporated in DPPC vesicles was performed in buffer B containing 100 mM NaCl, 0.2 mM Ca^{2+}, 5 mM Tris-HCl buffer (pH 7.4) at 25 °C with 10 μg/ml of SP-A. Fluorescence emission intensity was recoded from 300 to 554 nm after excitation at 282 nm. The slit widths were 4 nm for the excitation and emission beams.

SP-A Self-association Assay—Self-association assays of SP-A were performed as described previously (22, 36) by measuring the Ca^{2+}-dependent change in protein absorbance at 360 nm in a Beckman DU-640 spectrophotometer.

Re-LPS and Phospholipid Vesicle Aggregation Assays—DPPC/DPPG (7:3) (w/w) vesicles were prepared at a phospholipid concentration of 1 mg/ml by hydrating dry lipid films in a buffer containing 150 mM NaCl, 0.1 mM EDTA, 5 mM Tris-HCl (pH 7.4), and allowing them to swell for 1 h at 51 °C. Sonication, phosphorus determination, and vesicle-size analysis were performed as described above. Re-LPS was hydrated for 1 h at 41 °C in 5 mM Tris-HCl buffer (pH 7.4), containing 150 mM NaCl, and 0.1 mM EDTA and sonicated during 2 min.

LPS aggregation or DPPC/DPPG vesicle aggregation induced by SP-A was studied either at 25 or 37 °C by measuring the change in absorbance at 400 nm in a Beckman DU-640 spectrophotometer. SP-A-induced LPS aggregation assays were performed as described elsewhere (22, 23). Briefly, the sample and reference cuvettes were first filled with Re-LPS (40 μg/ml, final concentration) in 5 mM Tris-HCl buffer (pH 7.4), 150 mM NaCl, 0.2 mM EDTA. After a 10-min equilibration at 25 °C (or 37 °C), SP-A (20 μg/ml) was added to the sample cuvette, and the change in optical density at 400 nm was monitored. Next, Ca^{2+} (2.5 mM) was added to both the sample and reference cuvettes, and the change in absorbance was monitored again. Ca^{2+}-dependent LPS aggregation was reversed by adding EDTA (5 mM, final concentration). For SP-A-induced phospholipid vesicle aggregation assays, the final concentrations of SP-A, phospholipid, calcium, and EDTA were 20 μg/ml, 100 μg/ml, 2.5 mM, and 5 mM, respectively.

Adsorption Assay—The ability of recombinant SP-A1 and SP-$A1^{\Delta AVC,C6S}$ to enhance the adsorption of lipid extracts of porcine surfactants (LES) onto an air-liquid interface was performed on a Wilhelmy-like high sensitive surface microbalance, coupled to a small Teflon dish as previously reported (22). Lipid extracts of surfactant (LES), which contain surfactant lipids, SP-B, and SP-C, were prepared by chloroform/methanol extraction (37). The organic solvent was then evaporated to dryness under a stream of nitrogen, and traces of solvent were subsequently removed by evacuation under reduced pressure overnight. Multilamellar vesicles of LES were prepared by hydrating the dry proteolipid film in a buffer containing 150 mM NaCl, 25 mM Hepes, pH 6.9, and allowing them to swell for 1 h at 51 °C. After vortexing, the resulting multilamellar vesicles were used for the adsorption assay. Briefly, SP-A (7 μg/ml) was first added into the hypophase chamber of the Teflon dish, which contained 6 ml of 25 mM Hepes buffer, pH 6.9, 150 mM NaCl, and 5 mM $CaCl_2$. After LES injection (70 μg of phospholipids/ml) into the hypophase, phospholipid interfacial adsorption was measured following the change in surface tension as a function of time at 25 °C. Total phospholipid in LES was determined by phosphorus analysis.

Cell Assays—Monocyte-like U937 cells were grown in RPMI 1640 supplemented with 10% heat-inactivated fetal bovine serum (FBS), 2 mM glutamine, and penicillin G sodium (100 units/ml)/streptomycin sulfate (100 μg/ml), and 0.25 μg/ml amphotericin B under a 95% air-5% CO_2 humidified atmosphere at 37 °C. The medium was changed every 48 h. U937 cells were dispensed into 24-well plates at 1×10^6 cells/ml and differentiated into macrophages by incubation with 10 nM phorbol 12-myristate 13-acetate for 24 h at 37 °C in a 5% CO_2 humidified atmosphere. Then cells were washed with medium, and, 24 h later, cells were washed and pretreated with increasing concentrations (1–20 μg/ml) of SP-A for 10 min prior to 4-h Re-LPS (100 ng/ml) stimulation in the presence of 2% of heat-inactivated FBS at 37 °C. In another set of experiments, differentiated U937 cells were stimulated with smooth LPS (1 μg/ml), which hardly bound to SP-A. In some experiments, cells were pretreated with either 1 μg/ml anti-CD14 alone or in combination with SP-A for 10 min prior to 4-h LPS stimulation. Cell viability was confirmed by trypan blue exclusion.

For measurement of TNF-α production, cell-free culture supernatants were collected and assayed for TNF-α with an enzyme-linked immunoassay kit (OptEIA Set human TNF-α, BD Pharmingen). Four different cell cultures were used ($n = 4$). The assays from each U937 cell culture were performed in triplicate, the triplicate values were averaged, and their mean treated as a single point. The results are presented as the means (±S.E.), obtained by combining the results from each cell preparation. Results were expressed as a percentage of the level of TNF-α production by cells stimulated with LPS in the absence of SP-A.

For FITC-LPS binding assays, differentiated U937 cells (0.3×10^6 cells/ml) (96-well plates) were pretreated with 20 μg/ml SP-A for 10 min prior to 20-min FITC-LPS (1 μg/ml) incubation in the presence of 2% of heat-inactivated FBS at 37 °C. In some experiments, cells were pretreated with either 1 μg/ml anti-CD14 alone or in combination with SP-A for 10 min prior to 20-min FITC-LPS incubation. For measurement of cell-associated fluorescence, cultures were immediately washed three times with 300 μl of cold PBS. Then 100 μl of 0.2 mg/ml trypan blue in PBS were added to quench extracellular fluorescence, and the fluorescence intensity was measured in a Fluostar microplate reader at 485 nm excitation and 530 nm emission wavelength. Three different cell cultures were used, and the assays from each U937 cell culture were performed in quadruplicate. Results are presented as the means (±S.E.). For statistical analysis, mean comparison between groups was done by one-way analysis of variance followed by Bonferroni post hoc analysis; a confidence level of 95% or greater ($p < 0.05$) was considered significant.

RESULTS

Structural Characterization of SP-$A1^{\Delta AVC,C6S}$—Recombinant human SP-A1 and SP-$A1^{\Delta AVC,C6S}$ were expressed in CHO cells. Wild type recombinant SP-A1 had supratrimeric structure and was Asn^{187}-glycosylated and prolyl-hydroxylated (22). SP-$A1^{\Delta AVC,C6S}$ was efficiently secreted into the culture medium. Given its low binding affinity to a mannose-Sepharose affinity column in the presence of calcium, a new purification scheme was developed using anionic exchange, size exclusion, and hydrophobic interaction chromatography.

The NH_2-terminal sequences of SP-A1 and SP-$A1^{\Delta AVC,C6S}$ were determined by protein microsequencing. The results are summarized in Table I. SP-A1 showed three NH_2-terminal isoforms. Polypeptide subunits starting at position +1 (Glu) represented 50% of the protein, whereas isoforms with an additional Val^{-2}-Cys^{-1} (VC isoform) and Ala^{-3}-Val^{-2}-Cys^{-1} (AVC isoform) comprised 30 and 20%, respectively. In these three isoforms, the sequence of amino acids from positions +1 to +7 was identical to the reported NH_2-terminal sequence for human SP-A (SP-A1 or SP-A2). On the other hand, the combined mutant SP-$A1^{\Delta AVC,C6S}$ started at position +1 (Glu), and the sequence of amino acids to position +7 and beyond was identical to SP-A1, except for the substitution of Ser for Cys^6.

Oligomerization was assessed by size exclusion chromatography, electrophoresis under non-denaturing conditions, and electron microscopy. The recombinant expression of this construct in CHO K1 cells yielded SP-$A1^{\Delta AVC,C6S}$ in trimeric form (Fig. 1). Fig. 1 (*A* and *B*) show electron microscopy images of recombinant SP-A1 and SP-$A1^{\Delta AVC,C6S}$, respectively, using the rotatory shadowing technique. SP-A1 consisted of a heterogeneous population of supratrimeric oligomers (ranging from nonamers up to octadecamers) (Fig. 1*A*). In contrast, SP-$A1^{\Delta AVC,C6S}$ consisted of a homogeneous population of trimers. For some particles in side view, rod-like structures and globular domains are clearly observed (Fig. 1*B*). The rod-like structures would correspond to the neck domain, collagen-like region, and NH_2-terminal segments of the three polypeptide chains that form the trimer as it is graphically represented in Fig. 1. The trimeric structure of SP-$A1^{\Delta AVC,C6S}$ was confirmed by size exclusion chromatography (data not shown) and non-denaturing electrophoresis (without SDS or heat treatment)

TABLE I
Amino terminal sequence of recombinant human SP-A1 and SP-A1$^{\Delta AVC,C6S}$

Protein	Amino acid number[a]												Percentage[b]
	−3	−2	−1	1	2	3	4	5	6	7	8	9	10	
														%
SP-A1$^{\Delta AVC,C6S}$				E	V	K	D	V	S	V	G	S	Hyp[c]	100
SP-A1														
Sequence 1				E	V	K	D	V	C	V	G	S	Hyp	50
Sequence 2		V	C	E	V	K	D	V	C	V	G	S	Hyp	30
Sequence 3	A	V	C	E	V	K	D	V	C	V	G	S	Hyp	20

[a] Numbered according to the position in the reported native SP-A sequence.
[b] Calculated using the molecular yield (picomoles) of representative amino acids from each sequence divided by the molecular yield (picomoles) of total isoforms (e.g. % sequence 1 isoform = pmol sequence 1/pmol sequence 1 + pmol sequence 2 + pmol sequence 3).
[c] Hyp, hydroxyproline.

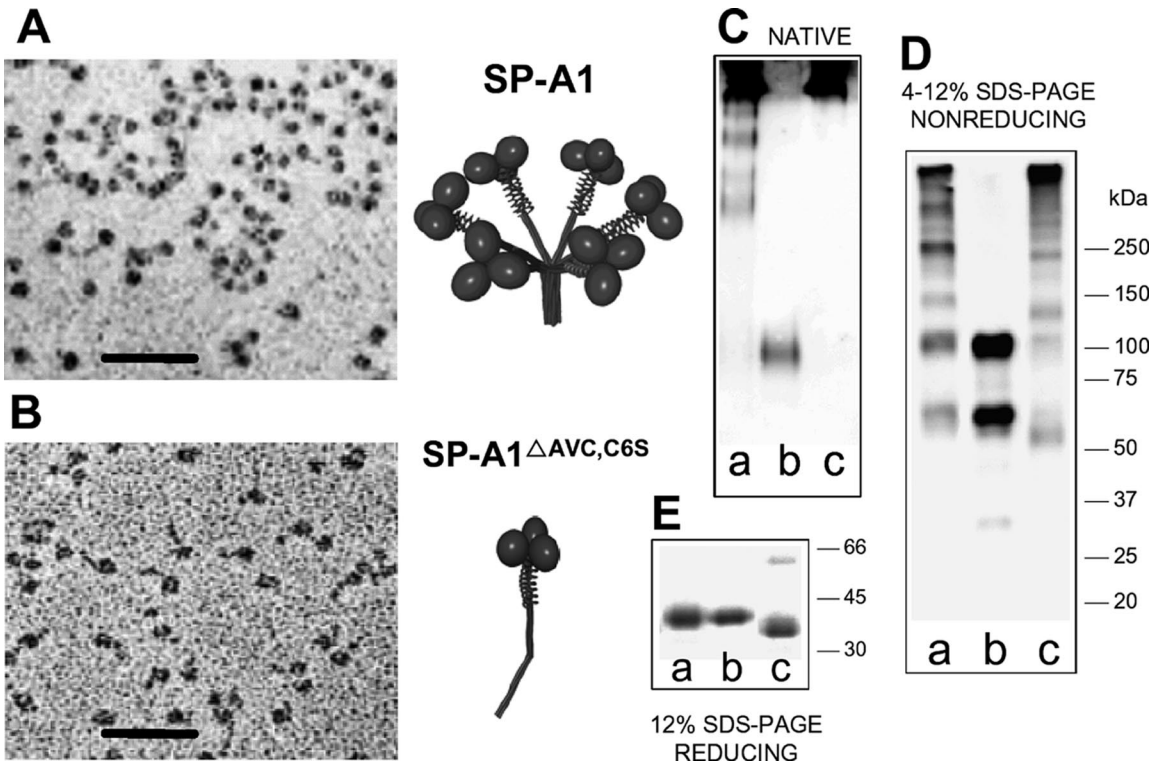

FIG. 1. *A* and *B*, electron micrographs after rotary shadowing of recombinant human SP-A1 and SP-A1$^{\Delta AVC,C6S}$, respectively, expressed in CHO K1 cells. The *bars* indicate a length of 50 nm. 25 ng of both SP-A1 and SP-A1$^{\Delta AVC,C6S}$ were subjected to electron microscopy as described in Ref. 31. The different degrees of oligomerization of SP-A1 and SP-A1$^{\Delta AVC,C6S}$ are also graphically represented. *C–E*, electrophoretic analysis of recombinant human SP-A1 (*lane a*), recombinant human SP-A1$^{\Delta AVC,C6S}$ mutant (*lane b*), and human SP-A from alveolar proteinosis patients (*lane c*). *C*, a Western blot after the separation of the SP-As on a 7% polyacrylamide gel under native conditions. The amount of each protein loaded was 100 ng. *D*, a Western blot after 4–12% SDS-PAGE under non-reducing conditions to identify disulfide-linked polypeptide chains. The amount of each protein loaded was 50 ng. In *E*, proteins (1 μg of each SP-A preparation) were subjected to 12% SDS-PAGE under reducing conditions and visualized by silver staining. *Numbers on the right* denote molecular mass.

under non-reducing conditions (Fig. 1*C*). This study corroborated that SP-A1$^{\Delta AVC,C6S}$ consisted of trimers (*lane b*), whereas wild-type SP-A1 (*lane a*) or natural SP-A isolated from alveolar proteinosis patients (*lane c*) consisted of supratrimeric oligomers.

To identify disulfide-linked polypeptide chains in SP-A1$^{\Delta AVC,C6S}$ trimers, we performed SDS gradient gel electrophoresis under non-reducing conditions (Fig. 1*D*). The trimeric SP-A1$^{\Delta AVC,C6S}$ (*lane b*) exhibited two major bands corresponding to two and three disulfide-linked chains, respectively, and a faint band corresponding to monomers. These results proved that part of the SP-A1$^{\Delta AVC,C6S}$ trimers contained two polypeptide chains covalently linked by at least one disulfide bond, and part of the SP-A1$^{\Delta AVC,C6S}$ trimers contained the three polypeptide chains cross-linked by two disulfide bonds. This indicates that Cys^{48} (located at the Pro-Cys-Pro-Pro interruption between the two collagen-like regions) as well as Cys^{65} (located at the C-terminal half of the collagen-like domain) contributed to these intra-trimer disulfide bonds. On the other hand, the composition of recombinant human SP-A1 (*panel D*, *lane a*) and natural human SP-A (*panel D*, *lane c*) revealed a ladder of different oligomeric forms ranging from dimers and trimers up to the octadecameric forms. *Panel E* (*lanes a* and *b*) shows that polypeptide chains of human SP-A1 and SP-A1$^{\Delta AVC,C6S}$ exhibited similar mobility as detected in SDS-PAGE under reducing conditions. The slight difference in mobility between monomeric recombinant forms (*lanes a* and *b*), and natural SP-A (*lane c*) was due to the higher degree of glycosylation in CHO K1 cells.

Fig. 2*A* shows that recombinant human SP-A1$^{\Delta AVC,C6S}$ trimers had circular dichroism (CD) spectra at low temperature comparable in shape and magnitude to published spectra for recombinant human SP-A1 and natural SP-A from healthy subjects or alveolar proteinosis patients (22). The thermal denaturation of the collagen triple helix of SP-A1$^{\Delta AVC,C6S}$, monitored by CD spectroscopy, is shown in Fig. 2*B* along with that of wild type SP-A1, which has been reported recently (22). The

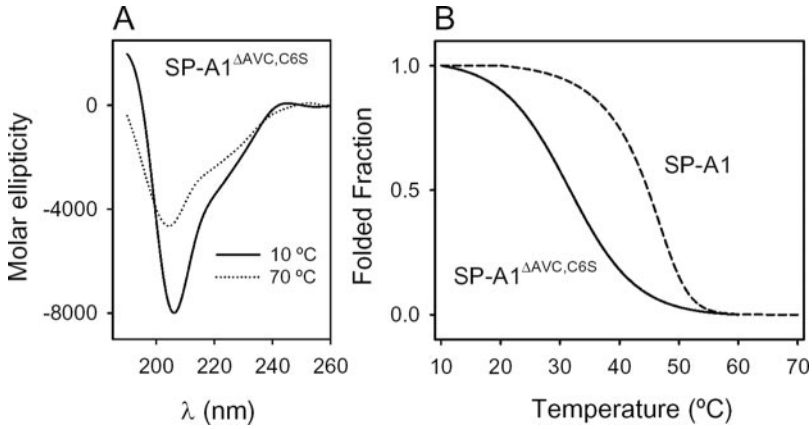

FIG. 2. *A*, circular dichroic spectra of SP-A1$^{\Delta AVC,C6S}$ at 10 and 70 °C in 5 mM Tris-HCl buffer, pH 7.4. *B*, unfolding curves of SP-A1 and SP-A1$^{\Delta AVC,C6S}$. Melting curves were monitored at 207 nm, at 120 μg of SP-A/ml, whereas the sample temperature was raised from 10 to 70 °C, with an average heating rate of 12 °C/h. The folded fraction (F) was calculated as described under "Experimental Procedures." The temperature where $F = 0.5$ was taken as the melting temperature (T_m). The results shown are from a representative one of three experiments.

collagen triple helix of SP-A1$^{\Delta AVC,C6S}$ melted at a midpoint temperature (T_m) of 32.7 ± 1 °C ($n = 3$). In contrast, the collagen triple helix of SP-A1 melted in a narrower temperature range than that of SP-A1$^{\Delta AVC,C6S}$ and at a midpoint temperature of 44.5 ± 0.3 °C ($n = 3$). Under physiological ionic conditions (in the presence of 1 mM calcium and 150 mM NaCl) the T_m of both SP-A1$^{\Delta AVC,C6S}$ and SP-A1 did not change significantly, showing T_m values of 33.3 ± 3.7 °C ($n = 3$) and 48.1 ± 3.6 °C ($n = 3$) for SP-A1$^{\Delta AVC,C6S}$ and SP-A1, respectively. Collectively, these data clearly indicated that a supratrimeric structure stabilized by NH_2-terminal disulfide bonds was important for the stabilization of the triple helix at physiological temperatures.

Next we examined the SP-A temperature-dependent susceptibility to trypsin degradation to further characterize the collagen triple helix stability of SP-A1$^{\Delta AVC,C6S}$ in comparison with wild type SP-A1. This technique was commonly used to characterize the effect of mutations on collagen triple helix stability in SP-D (25) and in type I collagen (38). The polypeptide chain of mature SP-A1 contains 20 trypsin cleavage targets; nine of them are located in the NH_2-terminal segment, collagen-like domain, and neck. Fig. 3 shows that both wild type SP-A1 and SP-A1$^{\Delta AVC,C6S}$ mutant were less susceptible to trypsin degradation following incubation at temperatures below their collagen melting temperatures (T_m) than above them. Thus, SP-A1$^{\Delta AVC,C6S}$ was much more susceptible than SP-A1 to trypsin degradation at 37 °C. These results are consistent with the finding that the collagen triple helix of the Cys^6 mutant was partially unfolded at 37 °C, which increased the susceptibility of the protein to proteolytic degradation. Fig. 3 also shows that the susceptibility to trypsin of wild type SP-A1 was similar at 25 and 37 °C (temperatures below its T_m: 44.5 °C) and was less than that of SP-A1$^{\Delta AVC,C6S}$ mutant at 25 °C, which suggests that the formation of the microfibrillar end piece of octadecamers restricts the accessibility of trypsin to some of its cleavage sites even more.

Binding of SP-A to Its Ligands—The binding of SP-A1 and SP-A1$^{\Delta AVC,C6S}$ to calcium was followed by changes in SP-A fluorescence emission intensity and by spectral shifts on excitation at 275 nm at 25 °C (Fig. 4*A*). The fluorescence of SP-A is dominated by the contribution of its two conserved tryptophan residues (29) located at positions 191 and 213 of the globular COOH-terminal domain. The two SP-A tryptophans are located near the calcium binding site (13), being sensitive markers of conformational changes in this region (22, 23, 36, 39).

Fig. 4*A* shows that SP-A1 and SP-A1$^{\Delta AVC,C6S}$ showed identical fluorescence emission spectra in the absence of calcium, suggesting the absence of abnormalities of the COOH-terminal end of the SP-A1$^{\Delta AVC,C6S}$ molecule. Upon addition of calcium, the fluorescence emission spectrum of both proteins showed an

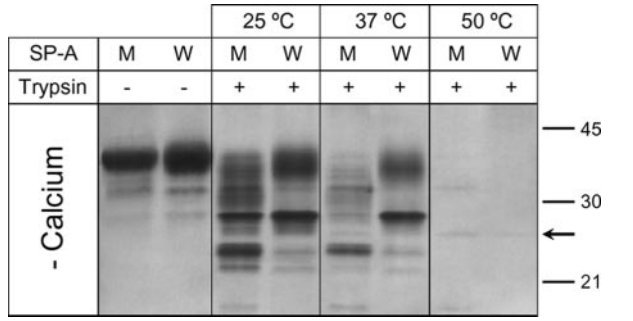

FIG. 3. **Protease sensitivity of wild type recombinant human SP-A1 (*W*) and the SP-A1$^{\Delta AVC,C6S}$ mutant (*M*) as a function of temperature.** The figure shows a silver-stained 12% reducing SDS-PAGE gel of SP-As incubated in the absence (−) or presence (+) of trypsin (SP-A/trypsin 15:1, w/w) for 30 min, in 5 mM Tris-HCl buffer, pH 7.4, at temperatures below and above the T_m of SP-A1$^{\Delta AVC,C6S}$ (32.7 °C) and SP-A1 (44.5 °C). *Numbers on the right* denote molecular mass. An *arrow* signals the position of trypsin (molecular weight, 23.8).

increase in fluorescence intensity accompanied by a blue-shift of the wavelength emission maximum from 330 (in the presence of EDTA) to 326 nm. This signified that the addition of calcium caused a conformational change in both proteins decreasing polarity in the environment of the tryptophan residues. The fact that both proteins showed similar fluorescence properties upon addition of calcium indicated that the degree of oligomerization did not affect the binding of calcium to the globular domains of SP-A. This was expected, because it was reported that calcium efficiently binds to the collagenase-resistant fragment of human SP-A (39).

The conformational change induced by calcium was also evaluated by protein susceptibility to trypsin degradation (Fig. 4*B*). Control experiments with serum albumin indicated that trypsin activity was not dependent on Ca^{2+} (data not shown). The binding of calcium to either SP-A1 or SP-A1$^{\Delta AVC,C6S}$ markedly decreased the extent of digestion of these proteins by trypsin in comparison with the extent of SP-A degradation in the absence of calcium (Fig. 3). These results suggest that the binding of calcium to its two binding sites in the globular head (13), and likely to a binding site outside the globular head (39), potentially located at a distinctive anionic patch between the collagen-like domain and the coiled-coil neck region (13), modifies protein conformation because the accessibility of trypsin cleavage targets of SP-A1 or SP-A1$^{\Delta AVC,C6S}$ was notably reduced. The presence of calcium also decreased the susceptibility to proteolysis of a collagenase-resistant fragment of human SP-A (39). Fig. 4*B* also shows that, in the presence of calcium, supratrimeric SP-A1 was more resistant to trypsin degradation than trimeric SP-A1$^{\Delta AVC,C6S}$, especially at 37 °C, a tempera-

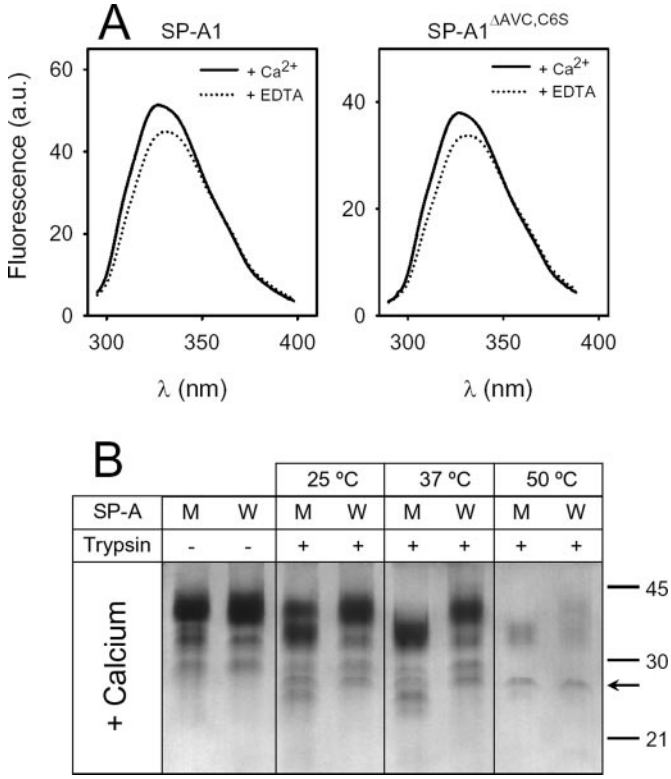

FIG. 4. *A*, fluorescence emission spectra of SP-A1 and SP-A1$^{\Delta AVC,C6S}$ in the presence of either 2 mM EDTA or 2 mM $CaCl_2$ at 25 °C. The binding of calcium to SP-As causes an increase in fluorescence intensity and a blue-shift of the wavelength emission maximum. *B*, effect of calcium on protease sensitivity of SP-A1 (*W*) and the SP-A1$^{\Delta AVC,C6S}$ mutant (*M*). SP-As were incubated in the absence (−) or presence (+) of trypsin (SP-A/trypsin 15:1, w/w) for 30 min, in 5 mM Tris-HCl buffer, pH 7.4, containing 1 mM $CaCl_2$ and 100 mM NaCl, at the indicated temperatures. The susceptibility of the SP-A to trypsin was analyzed by silver staining after separation on a 12% SDS-polyacrylamide gel under reducing conditions. The positions of molecular mass standards are indicated at the *right margin*. An *arrow* signals the position of trypsin.

ture at which the collagen domain of SP-A1$^{\Delta AVC,C6S}$ is partially unfolded (T_m: 33.3 °C in the presence of 1 mM calcium and 150 mM NaCl) and, therefore, the accessibility of trypsin to its cleavage sites at the collagen domain is greater.

The binding of SP-A to DPPC membranes was monitored as the fluorescence resonance energy transfer (FRET) from SP-A tryptophan residues (donor) to an appropriate acceptor such as a dansyl group located in the DPPC vesicle surface. This process is dependent on the proximity between donor and acceptor. The binding of different SP-As (natural SP-A, SP-A1, and SP-A1$^{\Delta AVC,C6S}$) to DPPC vesicles was determined on excitation at 282 nm while monitoring the increase of dansyl fluorescence as a result of FRET (Fig. 5*A*). Two types of experiments were done: (*a*) the DPPC/SP-A weight ratio was held constant while increasing the amount of dansyl-DHPE incorporated in DPPC vesicles (Fig. 5*B*) and (*b*) the dansyl-DHPE/DPPC ratio was held constant while increasing the DPPC/SP-A weight ratio (Fig. 5*C*). These experiments clearly indicated that SP-A1$^{\Delta AVC,C6S}$ was able to bind to DPPC vesicles. The binding increased as a function of mol% of dansyl group-incorporated in DPPC vesicles (Fig. 5*B*) and as a function of the DPPC/SP-A1$^{\Delta AVC,C6S}$ weight ratio (Fig. 5*C*) as was observed for either natural SP-A or wild type SP-A1. These results indicated that supratrimeric assembly was not essential for the binding of SP-A to phospholipid vesicles.

The binding of SP-A to rough-LPS in solution was followed by changes in FITC-Re-LPS fluorescence properties such as intensity and anisotropy (Fig. 6). FITC-Re-LPS has been widely used to study the interaction of LPS-binding proteins with rough-LPS (40, 41). Fig. 6*A* shows the time dependence of the fluorescence change when fluorescent rough-LPS (4×10^{-7} M) reacts with a 3.5-fold excess of either SP-A1 or SP-A1$^{\Delta AVC,C6S}$ (13.8×10^{-7} M, considering the molecular weight of SP-A monomer). The magnitude of the fluorescence change after SP-A addition clearly increased with higher degree of oligomerization. Control experiments were done with free fluorescein to demonstrate that all of these changes did not result from the interaction of the different SP-As with the dye (fluorescein), but with the LPS molecule (data not shown). We also examined the binding of different SP-As to FITC-Re-LPS by measuring fluorescence anisotropy of the fluorescently labeled LPS molecule (Fig. 6*B*). Fluorescence anisotropy measurements depend on the rate and extent of the rotational motion of the fluorophore during the lifetime of the excited state. FITC-Re-LPS possessed an emission anisotropy of around 0.067 ± 0.003 (λx = 470 nm; λm = 520 nm) in 5 mM Tris-HCl buffer, pH 8, containing 100 mM NaCl, 1 mM EDTA, at 25 °C. The formation of FITC-Re-LPS/SP-A complexes led to a significant increase of fluorescence emission anisotropy, indicating that the binding of SP-A1 or SP-A1$^{\Delta AVC,C6S}$ to Re-LPS caused mechanical restrictions of the rotational mobility of the dye. The higher increase in anisotropy of FITC-Re-LPS bound to SP-A1 could be attributed to a more restricted movement of the labeled LPS molecule when it is bound to supratrimeric SP-A1. Control experiments with free fluorescein indicated that the SP-A-induced increase in FITC-Re-LPS fluorescence anisotropy was due to the binding of SP-A to Re-LPS but not to the fluorescent probe.

SP-A Self-association and SP-A-induced Ligand Aggregation—Fig. 7*A* shows that the cysteine mutant does not self-associate in the presence of calcium at 25 °C (or 37 °C), indicating that a supratrimeric assembly is needed for this activity. In addition, SP-A1$^{\Delta AVC,C6S}$ did not induce Re-LPS aggregation (Fig. 7*B*) and phospholipid vesicle aggregation (Fig. 7*C*) despite the fact that SP-A1$^{\Delta AVC,C6S}$ was able to bind to both Re-LPS and phospholipids. These data strongly suggest that the ability of SP-A to induce Re-LPS and phospholipid vesicle aggregation might correlate with the capability of SP-A to self-associate in the presence of calcium. All of these processes required the protein to be in a supratrimeric assembly.

SP-A-induced Enhancement of Surfactant Interfacial Adsorption Rate—Fig. 8 shows the change in surface pressure as a function of time for reconstituted surfactant-like membranes (containing SP-B and SP-C) in the absence and presence of SP-A1 and SP-A1$^{\Delta AVC,C6S}$. SP-A1$^{\Delta AVC,C6S}$ poorly affected the interfacial adsorption rate of surfactant-like membranes. In contrast, SP-A1 highly enhanced the adsorption rate, reaching the equilibrium surface pressure (47 millinewtons/m) at 20 min, as previously reported (22). Much longer times would be needed to reach the equilibrium surface pressure for reconstituted lipid extract alone or in the presence of SP-A1$^{\Delta AVC,C6S}$. These results revealed that the SP-A-induced enhancement of surfactant interfacial adsorption is dependent on the supratrimeric structure of SP-A.

SP-A-induced Inhibition of TNF-α Production by Rough or Smooth LPS-stimulated U937 Cells—To investigate the effect of the degree of oligomerization on the anti-inflammatory activity of SP-A, increasing amounts (1–20 μg/ml) of recombinant forms of human SP-A (SP-A1 and SP-A1$^{\Delta AVC,C6S}$) were preincubated with macrophage-like cells 10 min prior to 4-h activation with an optimal concentration of rough-LPS (100 ng/ml) (Fig. 9*A*). An appropriate amount of heat-inactivated FBS (2%) was included in the medium. The inhibitory effect of SP-A1 and SP-A1$^{\Delta AVC,C6S}$ upon rough LPS-induced TNF-α secretion depended upon the SP-A concentrations. Concentrations as low

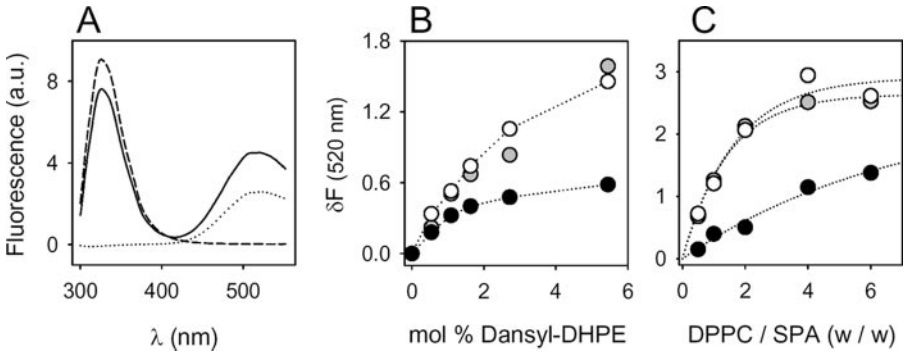

FIG. 5. **Interaction of natural SP-A, SP-A1, and SP-A1$^{\Delta AVC,C6S}$ with DPPC vesicles monitored by FRET between SP-A tryptophan residues and dansyl groups located in DPPC vesicle surface.** The tryptophan residues were excited at 282 nm, and fluorescence was monitored between 300 and 554 nm. *A*, fluorescence emission spectra of SP-A in the absence (*dashed line*) and presence (*solid line*) of dansyl-DPPC vesicles. The fluorescence emission spectrum of dansyl-DPPC vesicles in the absence of SP-A (*dotted line*) is also shown. The binding of SP-A to dansyl- DPPC vesicles can be monitored by the increase of dansyl fluorescence on excitation at 282 nm. *B*, the increase of dansyl fluorescence as a function of mol % dansyl-DHPE incorporated in DPPC vesicles (DPPC/SP-A 4:1, w/w). *C*, the increase of dansyl fluorescence as a function of DPPC/SP-A weight ratio. Experiments were performed with natural SP-A (*gray circles*), SP-A1 (*open circles*), and SP-A1$^{\Delta AVC,C6S}$ (*closed circles*). A representative experiment of three experiments is shown.

FIG. 6. **Binding of SP-A to Re-LPS monitored by changes in FITC-Re-LPS fluorescent properties.** *A*, the time dependence of the fluorescence change when FITC-Re-LPS reacts with SP-A1 and SP-A1$^{\Delta\ \Delta VC,C6S}$ in 100 mM NaCl, 1 mM EDTA, 5 mM Tris-HCl buffer, pH 8, at 25 °C. The results shown are from a representative one of three experiments. *B*, wild type SP-A1 (*W*) (*open bar*) and SP-A1$^{\Delta AVC,C6S}$ mutant (*M*) (*closed bar*) induce an significant increase in fluorescence anisotropy upon binding to FITC-Re-LPS in 100 mM NaCl, 1 mM EDTA, 5 mM Tris-HCl buffer, pH 8, at 25 °C. Similar results were found when the buffer contained 1 mM Ca^{2+} (data not shown). All data points are the mean values of experiments performed in triplicate ± S.D. *, $p < 0.05$ *versus* control.

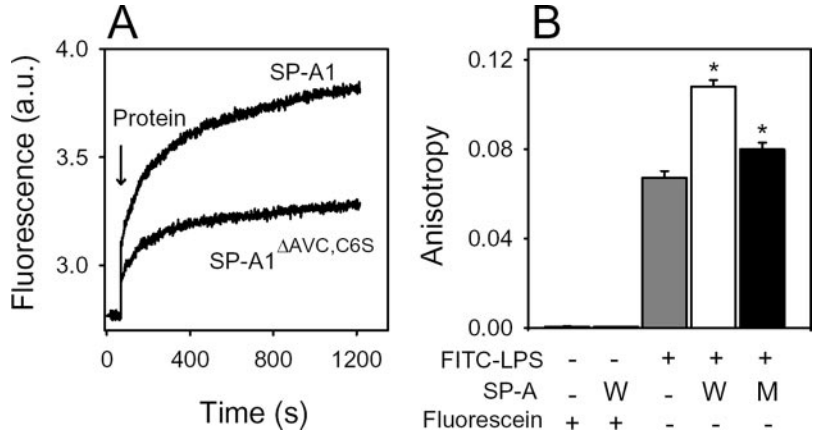

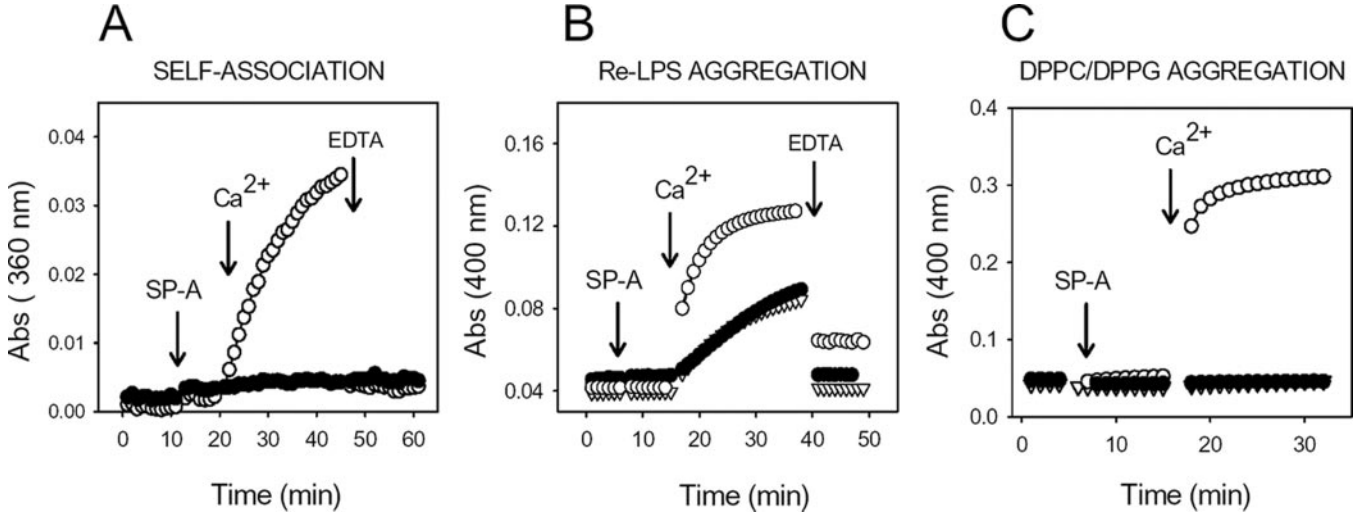

FIG. 7. *A*, kinetics of Ca^{2+}-dependent self-association of SP-A1 (○) and SP-A1$^{\Delta AVC,C6S}$ (●). Recombinant human SP-As (20 μg/ml) were added to the sample cuvette filled with 5 mM Tris-HCl buffer (pH 7.4). The turbidity change at 360 nm was monitored at 25 °C (or 37 °C) at 1-min intervals. After stabilization, 5 mM Ca^{2+} (final concentration) was added to both the sample and reference cuvette, and the turbidity changes monitored again. Addition of EDTA (10 mM, final concentration) dissociated SP-A1 aggregates induced by Ca^{2+}. *B*, kinetics of Ca^{2+}-dependent Re-LPS aggregation in the absence (▽) or presence of SP-A1 (○) and SP-A1$^{\Delta AVC,C6S}$ (●). The experiments were done as described under "Experimental Procedures" in 5 mM Tris-HCl buffer (pH 7.4), 150 mM NaCl, at 25 °C. The final concentrations of SP-A, Re-LPS, calcium, and EDTA were 20 μg/ml, 40 μg/ml, 2.5 mM, and 5 mM, respectively. *C*, kinetics of DPPC/DPPG vesicle aggregation induced by SP-A in the presence of calcium. Experiments with vesicles alone (▽) or in the presence of SP-A1 (○) and SP-A1$^{\Delta AVC,C6S}$ (●) are shown. The experiments were done as described under "Experimental Procedures" in 5 mM Tris-HCl buffer (pH 7.4), 150 mM NaCl, at 25 °C. The final concentrations of SP-A, DPPC/DPPG vesicles, and calcium were 20 μg/ml, 100 μg/ml, and 2.5 mM, respectively. In *A–C* one representative experiment of three experiments is shown.

as 5 μg/ml of either supratrimeric SP-A1 or trimeric SP-A1$^{\Delta AVC,C6S}$ significantly inhibited TNF-α production by about 90 and 49%, respectively. None of these SP-As alone had any effect on TNF-α production by resting differentiated U937 cells for 4 h after SP-A addition (data not shown). The inhibitory effect of SP-A1 on LPS-induced TNF-α secretion was similar to

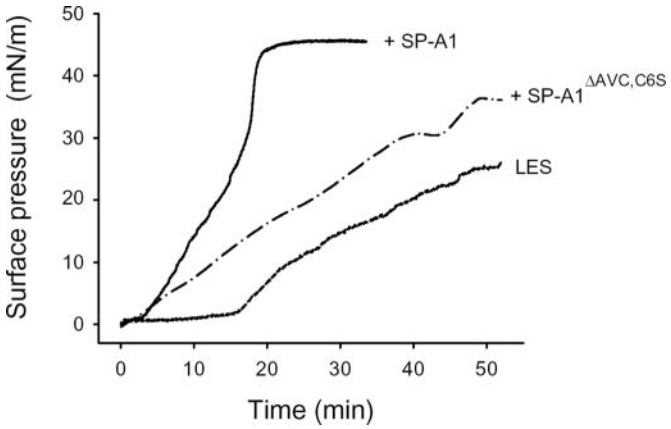

FIG. 8. **Effect of SP-A1 and SP-A1$^{\Delta AVC,C6S}$ on the adsorption kinetic of lipid extracts of surfactant (*LES*) onto the air-liquid interface.** Phospholipid interfacial adsorption was measured at 25 °C following the change in surface pressure as a function of time for samples containing 70 μg of phospholipids/ml, with or without either SP-A1 or SP-A1$^{\Delta AVC,C6S}$ (7 μg/ml), in 5 mM Hepes buffer, pH 7.0, containing 150 mM NaCl, and 5 mM $CaCl_2$. One representative experiment of three experiments is shown.

that of 1 μg/ml 28C5, an anti-CD14 antibody that has been shown to block Re-LPS binding to CD14 (41, 42) (data not shown).

To determine whether part of the anti-inflammatory effect of SP-A1 could be due to the ability of SP-A1, but not of SP-A1$^{\Delta AVC,C6S}$, to induce Re-LPS aggregation in the presence of calcium, which would reduce LPS toxicity (43), we also used a smooth serotype of LPS to stimulate macrophage-like U937 to which SP-A hardly binds (44). Fig. 9*B* shows that concentrations of both SP-A1 and SP-A1$^{\Delta AVC,C6S}$ equal to or higher than 5 μg/ml inhibited smooth LPS-induced TNF-α production by about 90 and 69%, respectively. Together, these results indicate that the anti-inflammatory activity of SP-A requires only assembly of a trimer.

On the other hand, our results on the effect of SP-A on the membrane binding of FITC-LPS by differentiated U937 coincided with those of Stamme *et al.* (45), who found that human SP-A significantly decreased association of rough [^{3}H]Rb-LPS to mCD14-transfected HEK cells in the presence of 5% serum. Fig. 10 shows that both SP-A1 and SP-A1$^{\Delta AVC,C6S}$ equally decreased the fluorescence associated to macrophage-like U937 cells by 80% in the presence of 2% serum. Anti-CD14–28C5 (1 μg/ml), which has been shown to mask the LPS binding site on CD14 (41, 42), similarly hampered the FITC-LPS binding to U937 cells. These data suggest that the SP-A-induced inhibition of smooth or rough LPS inflammatory response might be, at least in part, mediated by blocking the binding of LPS to its cellular receptor complex.

DISCUSSION

The aim of this study was to investigate the effect of the degree of oligomerization on the structural and functional properties of mammalian cell-derived human SP-A1. To obtain human SPA1 trimers, the cysteine at position +6 of human SP-A1 was removed by site-directed mutagenesis (serine was substituted for cysteine 6), and the cysteinyl isoforms (containing Cys^{-1}) were abolished by replacing SP-A1 signal sequence with human IgG light-chain signal sequence. The rationale for this strategy is based on the fact that individual rat SP-A disruption of Cys^6 (17) or Cys^{-1} (18) by substitution with Ser did not prevent the assembly of supratrimeric SP-A as detected by cross-linking analyses and gel exclusion chromatography. In addition, it is thought that at least two or three cysteine residues have to be present in the NH_2-terminal domain of collectins (mannose-binding protein-A, conglutinin, SP-D, and rat SP-A) to form disulfide-linked supratrimeric oligomers (17, 18, 25, 26, 46). However, there are some departures from this assumption: CL-43 is secreted as a trimer despite having two NH_2-terminal cysteine residues in exactly the same positions as SP-D (Cys^{15} and Cys^{20}); and canine SP-A, which has only one NH_2-terminal cysteine residue (Cys^6), assembles into higher oligomers. The mechanism by which trimers assemble into larger oligomers is still unclear. It is believed that, besides the number of NH_2-terminal cysteines, residues within the NH_2-terminal segment and the NH_2-terminal region of the collagen-like domain might also contribute to the oligomerization of trimeric subunits (46–48).

The combined mutation used in this study eliminates potential sites of inter-chain disulfide cross-linking within the most NH_2-terminal portion of human SP-A. The analysis of the NH_2-terminal sequence of recombinant forms of human SP-A1 indicates that the combined mutant SP-A1$^{\Delta AVC,C6S}$ started at position +1 (Glu) of the reported NH_2-terminal sequence for human SP-A, whereas SP-A1 was composed of Cys^{-1} isoforms which contained amino acid extensions derived from its signal peptide. Polypeptide subunits of SP-A1 starting at Glu^1 represent 50% of the protein, whereas isoforms containing Cys^{-1} (VC and AVC isoforms) represent the remaining 50%. Cys^{-1} may contribute to the supratrimeric assembly by intra- or intertrimer disulfide cross-linking in the NH_2-terminal portion of the molecule.

The recombinant expression of this combined mutant in mammalian CHO K1 cells yielded SP-A1$^{\Delta AVC,C6S}$ in trimeric form, identified by size exclusion chromatography, electron microscopy, and non-denaturing electrophoresis. Electron microscopy showed that SP-A1$^{\Delta AVC,C6S}$ assembled as a single arm of the supratrimeric recombinant human SP-A1 molecule, which consisted of octadecamers (six-armed), dodecamers (four-armed), and nonamers (three-armed). These results suggest that disulfide bonds at the NH_2-terminal segment of human SP-A seem to be required for the formation of oligomers of trimeric subunits. In the case of mammalian cell-derived mannose-binding protein-A, individual disruption of Cys^6 by substitution with Ser yielded mainly trimers but also hexamers and low levels of higher oligomers, indicating that other cysteine residues (Cys^{13} and Cys^{18}) at the NH_2-terminal segment also contribute to the supratrimeric assembly by intra- or intertrimer disulfide cross-linking (46). On the other hand, the two cysteines of the NH_2-terminal segment of rat SP-D (Cys^{15} and Cys^{20}) seem to be required for the SP-D supratrimeric assembly into dodecamers (25).

Polypeptide chains of SP-A1$^{\Delta AVC,C6S}$ and SP-A1 have identical mobility in SDS-PAGE under reducing conditions. Likewise, disulfide-linked trimers and dimers of SP-A1$^{\Delta AVC,C6S}$ and SP-A1 have identical mobility on 4–12% SDS-PAGE under nonreducing conditions. SP-A1$^{\Delta AVC,C6S}$ trimers have fluorescence and circular dichroism spectra comparable to those of supratrimeric SP-A1, indicating that trimeric SP-A1$^{\Delta AVC,C6S}$ has structural characteristics similar to supratrimeric SP-A1. However, we found that the collagen triple helix of the cysteine mutant melted at lower temperature (32.7 °C) than that of SP-A1, whose T_m is 44.5 (22). Both proteins, SP-A1$^{\Delta AVC,C6S}$ and SP-A1, were much more resistant to trypsin degradation at temperatures below their collagen melting temperatures than above them. Consistently, the trypsin susceptibility of SP-A1$^{\Delta AVC,C6S}$ was greater than that of wild type SP-A1 at 37 °C. These results suggest that the lack of the supratrimeric assembly would yield to a partly unfolded SP-A at physiological temperatures that would be more susceptible to proteolytic degradation. Similar results were found with recombinant rat

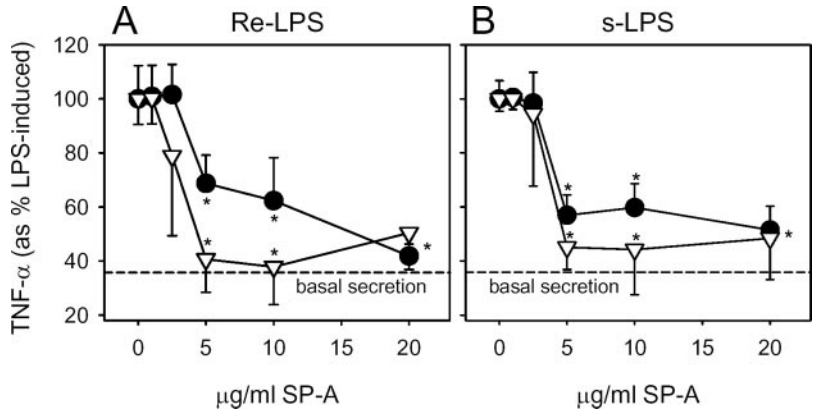

FIG. 9. **SP-A-induced inhibition of TNF-α production by macrophage-like U937 cells stimulated with rough (*A*) or smooth (*B*) LPS.** Differentiated U937 cells (1×10^6 cells/ml) were preincubated in the absence or presence of various concentrations of either SP-A1 (*open triangles*) or SP-A1$^{\Delta AVC,C6S}$ (*closed circles*) for 10 min prior to 4 h activation with either 100 ng/ml rough-LPS (*A*) or 1 μg/ml smooth-LPS (*B*), in the presence of 2% fetal bovine serum, at 37 °C. Cell-free supernatants were collected at 4 h after LPS treatment, and the levels of TNF-α were measured by using an enzyme-linked immunosorbent assay kit. Data presented are from four different cell cultures ($n = 4$). The assays from each U937 cell culture were performed in triplicate, the triplicate values were averaged, and their mean treated as a single point. The results are presented as the means (±S.E.). Results were expressed as a percentage of LPS-induced TNF-α levels. *, $p < 0.05$ compared with response elicited by LPS in the absence of SP-A.

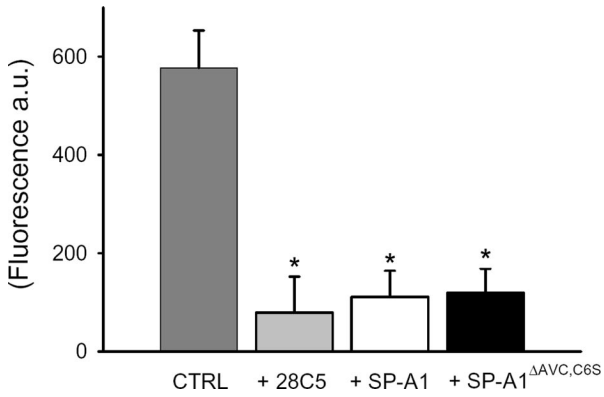

FIG. 10. **Effect of SP-A1 and SP-A1$^{\Delta AVC,C6S}$ on FITC-LPS binding by macrophage-like U937 cells.** Differentiated U937 cells (0.3×10^6 cells/ml) were preincubated in the absence (*gray bar*) or presence of either 1 μg/ml anti-CD14 (28C5) (*shaded bar*), 20 μg/ml SP-A1 (*open bar*), or 20 μg/ml SP-A1$^{\Delta AVC,C6S}$ (*closed bar*) for 10 min prior to 20-min incubation with FITC-LPS (1 μg/ml) in the presence of 2% of heat-inactivated FBS, at 37 °C. For measurement of cell associated fluorescence, cultures were immediately washed three times with 300 μl of cold PBS, and then with 100 μl of 0.2 mg/ml trypan blue in PBS. Fluorescence emission intensity was measured at 485 nm excitation and 530 nm emission wavelengths. Data presented are from three different cell cultures. The assays from each U937 cell culture were performed in quadruplicate. The results are presented as the means (± S.E.). *, $p < 0.05$ *versus* control.

SP-D expressed in mammalian cells. A mutation of the NH_2-terminal cysteines at positions 15 and 20 resulted in the production of trimers, with increased susceptibility to proteolytic degradation at 37 °C (25). It is possible that oxidative cleavage of disulfide bonds at the NH_2-terminal segment, by exposing the lungs to environmental pollutants (*e.g.* ozone, SO_2, or nitrogen oxides), affects the supratrimeric assembly of SP-A or SP-D along with other conformational changes.

SP-A binds to phospholipid vesicles that contain DPPC, and the major lipid binding site resides in the globular domain (2, 12, 13). The capability of SP-A1$^{\Delta AVC,C6S}$, SP-A1, and natural human SP-A to bind to DPPC vesicles was analyzed by fluorescence resonance energy transfer from SP-A tryptophan residues to a dansyl group located in the DPPC vesicle surface. These analyses indicated that supratrimeric assembly was not essential for the binding of SP-A to phospholipids. Importantly, the trimeric SP-A1$^{\Delta AVC,C6S}$ was unable to induce phospholipid vesicle aggregation in the presence of calcium despite the fact that this protein was able to bind to phospholipids and calcium. These results indicate that Ca^{2+}-dependent phospholipid vesicle aggregation induced by human SP-A requires the protein to be in a supratrimeric assembly.

The mechanism involved in the vesicle aggregation phenomenon is poorly understood. It is likely that vesicle aggregation activity of human SP-A is related to the ability of the highly multimerized protein to cross-link different vesicles. At the same time, the ability of human SP-A to self-associate in the presence of calcium would greatly increase the vesicle aggregation activity of SP-A. Here we demonstrated that the cysteine mutant did not undergo self-association in the presence of calcium, and it was unable to induce aggregation of membranes, which supports the concept that both processes are related phenomena. Haagsman *et al.* (39) proposed that the lipoprotein aggregation induced by calcium could be mediated by Ca^{2+}-induced self-association of human SP-A molecules. In addition, we found that the calcium activation constant (K_a^{Ca2+}) for both processes is similar at physiological ionic strength and is in the range of 1–2 μM (33, 36). Our current understanding is that calcium causes conformational changes in the globular domain of SP-A detected by fluorescence spectroscopy (22, 36, 39) and transmission electron microscopy (49). We propose a model for self-association of supratrimeric SP-A in which, upon binding to Ca^{2+}, protein association occurs among adjacent globular heads and nearby regions provided that a supratrimeric assembly and a structurally intact collagen domain (22, 36) ensure the correct grouping and orientation of globular heads in the oligomer. Self-associated SP-A molecules would connect surfactant membranes by interaction of their globular heads with membrane surfaces of contiguous bilayers. SP-A protein networks interacting with monolayers of surfactant phospholipids are visible by transmission electron microscopy (50) or epifluorescence microscopy (51). This type of calcium-dependent supraquaternary organization of supratrimeric SP-A and cooperative interaction with surfactant membranes could stabilize large surfactant aggregates, decrease surfactant inactivation in the presence of serum protein inhibitors, and facilitate interfacial adsorption of surfactant.

Related to the ability of SP-A to enhance the interfacial adsorption rate of surfactant-like membranes, the results presented here revealed that SP-A1$^{\Delta AVC,C6S}$ did not promote the spreading of SP-B/SP-C-surfactant membranes along the surface. These results support the idea that the capability of SP-A

to self-associate and to induce phospholipid aggregation predicts the surface active properties of the protein in concerted action with SP-B (28). Collectively, our results suggest that surfactant-related activities of SP-A depend on the supratrimeric assembly of the protein. Consistent with this assumption is a recent *in vivo* study that indicates that the SP-A collagen-deficient mutant expressed in the lungs of SP-A null (SP-$A^{-/-}$) mice converts SP-A into an inhibitor of surfactant function (52). *In vitro* studies show that the collagen-deficient mutant of SP-A is expressed as a trimer (53), suggesting that the collagen-like region and/or supratrimeric assembly play an important role in the accommodation of SP-A in the alveolar lipid-rich fluid.

The large excess of SP-A and SP-B/SP-C-surfactant membranes in the lung air spaces minimizes the biological effects of endotoxins, such as LPS, or microbes that enter the alveolus. SP-A binds to rough LPS and induces rough-LPS aggregation in the presence of calcium (44). Aggregation of LPS reduces LPS toxicity (43) and facilitates phagocytosis by alveolar macrophages (54). We found that the binding of human SP-A to FITC-Re-LPS increased with the degree of oligomerization, but supratrimeric assembly was not essential. Despite the ability of trimeric SP-$A1^{\Delta AVC,C6S}$ to bind to Re-LPS, this mutant was unable to induce Re-LPS aggregation in the presence of calcium, indicating that the supratrimeric assembly of SP-A is required for this activity. We propose that Re-LPS or bacteria aggregation induced by SP-A is enhanced by SP-A self-association dependent on calcium. Accordingly, self-associated SP-A would bind to endotoxins or bacteria by the globular heads, resulting in bacterial aggregation, whereas the collagen tails of these aggregates would be free to interact with receptors on the surface of macrophages initiating phagocytosis and inflammatory responses (9). Moreover, Gardai *et al.* (9) suggested that significant self-association of SP-A is required for the optimal stimulation of macropinocytosis induced by interaction of SP-A collagen tails with the calreticulin/CD91 system on the surface of phagocytic cells. Results indicated that agglutination and phagocytosis of inhaled pathogens or toxins mediated by SP-A might depend on the supratrimeric assembly of the protein.

We also have analyzed the effect of the degree of oligomerization on the anti-inflammatory activity of SP-A, which is responsible for maintaining low alveolar inflammation in the resting lung by causal stimuli such as low concentrations of inhaled LPS. We found that both SP-A1 and SP-$A1^{\Delta AVC,C6S}$, at concentrations equal to or higher than 5 μg/ml, significantly inhibited TNF-α production by macrophage-like cells stimulated by either rough LPS, to which they bind, or smooth LPS, to which they hardly bind. In addition, both SP-A1 and SP-$A1^{\Delta AVC,C6S}$ hampered the binding of FITC-LPS to macrophage-like U937 cells in a manner similar to anti-CD14–28C5, an anti-CD14 antibody that has been shown to block Re-LPS binding to CD14 (41, 42). Altogether, these data indicate that supratrimeric assembly of SP-A was not required for the anti-inflammatory effects of SP-A. SP-A-induced inhibition of smooth or rough LPS inflammatory response might be, at least in part, mediated by blocking the binding of LPS to its cellular receptor complex since SP-A binds to CD14 by its neck domain (55). Alternatively, SP-A, through its globular heads, could bind to signal inhibitory regulatory protein α, expressed by mononuclear phagocytes, to initiate a signal pathway that blocks pro-inflammatory cytokine production as recently reported by Gardai *et al.* (9).

In summary, this study indicated for the first time that a supratrimeric assembly of human SP-A was important for the thermal stability of the protein at physiological temperatures and SP-A protection against trypsin degradation. SP-A supratrimeric assembly was essential for Ca^{2+}-dependent SP-A self-association, SP-A-induced aggregation of phospholipid vesicles and LPS micelles, and SP-A-promoted adsorption of SP-B/SP-C-surfactant membranes to an air-liquid interface. However, supratrimeric assembly was not essential for the role of SP-A in the inhibition of rough or smooth LPS inflammatory response, which likely involves SP-A binding to cellular receptors by its globular and/or neck domains (9, 55).

Acknowledgments—We acknowledge Dr. F. U. Bosch from ALTANA Pharma for strong advice and support on the purification of SP-$A1^{\Delta AVC,C6S}$ and Jens Breyer for excellent assistance in preparing SP-$A1^{\Delta AVC,C6S}$ and SPA1. We also thank Dr. Peter Tobias, from the Scripps Research Institute, La Jolla, CA, for providing monoclonal antibody anti-CD14 (28C5), and Dr. Kevan Hartshorn, from Boston University School of Medicine, and Dr. Frank X. McCormack, from the University of Cincinnati School of Medicine, for useful comments and suggestions from a critical reading of the manuscript.

REFERENCES

1. McCormack, F. X., and Whitsett, J. A. (2002) *J. Clin. Invest.* **109,** 707–712
2. Casals, C. (2001) *Pediatr. Pathol. Mol. Med.* **20,** 249–268
3. Hawgood, S., and Poulain, F. R. (2001) *Annu. Rev. Physiol.* **63,** 495–519
4. Wu, H., Kuzmenko, A., Wan, S., Schaffer, L., Weiss, A., Fisher, J. H., Kim, K. S., and McCormack, F. X. (2003) *J. Clin. Invest.* **111,** 1589–1602
5. McCormack, F. X., Gibbons, R., Ward, S. R., Kuzmenko, A., Wu, H., and Deepe, G. S., Jr. (2003) *J. Biol. Chem.* **278,** 36250–36256
6. Lu, J., Teh, C., Kishore, U., and Reid, K. B. (2002) *Biochim. Biophys. Acta* **1572,** 387–400
7. Crouch, E., and Wright, J. R. (2001) *Annu. Rev. Physiol.* **63,** 521–554
8. van de Wetering, J. K., van Golde, L. M., and Batenburg, J. J. (2004) *Eur. J. Biochem.* **271,** 1229–1249
9. Gardai, S. J., Xiao, Y. Q., Dickinson, M., Nick, J. A., Voelker, D. R., Greene, K. E., and Henson, P. M. (2003) *Cell* **115,** 13–23
10. LeVine, A. M., Bruno, M. D., Huelsman, K. M., Ross, G. F., Whitsett, J. A., and Korfhagen, T. R. (1997) *J. Immunol.* **158,** 4336–4340
11. LeVine, A. M., Whitsett, J. A., Gwozdz, J. A., Richardson, T. R., Fisher, J. H., Burhans, M. S., and Korfhagen, T. R. (2000) *J. Immunol.* **165,** 3934–3940
12. McCormack, F. X. (1998) *Biochim. Biophys. Acta* **1408,** 109–131
13. Head, J. F., Mealy, T. R., McCormack, F. X., and Seaton, B. A. (2003) *J. Biol. Chem.* **278,** 43254–43260
14. Floros, J., and Hoover, R. R. (1998) *Biochim. Biophys. Acta* **1408,** 312–322
15. Hoppe, H. J., Barlow, P. N., and Reid, K. B. (1994) *FEBS Lett.* **344,** 191–195
16. Wallis, R., and Drickamer, K. (1997) *Biochem. J.* **325,** 391–400
17. McCormack, F. X., Pattanajitvilai, S., Stewart, J., Possmayer, F., Inchley, K., and Voelker, D. R. (1997) *J. Biol. Chem.* **272,** 27971–27979
18. Elhalwagi, B. M., Damodarasamy, M., and McCormack, F. X. (1997) *Biochemistry* **36,** 7015–7025
19. Voss, T., Eistetter, H., Schafer, K. P., and Engel, J. (1988) *J. Mol. Biol.* **201,** 219–227
20. Haas, C., Voss, T., and Engel, J. (1991) *Eur. J. Biochem.* **197,** 799–803
21. Wang, G., Bates-Kenney, S. R., Tao, J. Q., Phelps, D. S., and Floros, J. (2004) *Biochemistry* **43,** 4227–4239
22. Garcia-Verdugo, I., Sanchez-Barbero, F., Bosch, F. U., Steinhilber, W., and Casals, C. (2003) *Biochemistry* **42,** 9532–9542
23. Garcia-Verdugo, I., Wang, G., Floros, J., and Casals, C. (2002) *Biochemistry* **41,** 14041–14053
24. Tuner, M. W. (2003) *Mol. Immunol.* **40,** 423–429
25. Brown-Augsburger, P., Hartshorn, K., Chang, D., Rust, K., Fliszar, C., Welgus, H. G., and Crouch, E. C. (1996) *J. Biol. Chem.* **271,** 13724–13730
26. Zhang, P., McAlinden, A., Li, S., Schumacher, T., Wang, H., Hu, S., Sandell, L., and Crouch, E. (2001) *J. Biol. Chem.* **276,** 19862–19870
27. Hickling, T. P., Malhotra, R., and Sim, R. B. (1998) *Mol. Med.* **4,** 266–275
28. Hawgood, S., Benson, B. J., Schilling, J., Damm, D., Clements, J. A., and White, R. T. (1987) *Proc. Natl. Acad. Sci. U. S. A.* **84,** 66–70
29. Casals, C., Miguel, E., and Perez-Gil, J. (1993) *Biochem. J.* **296,** 585–593
30. Hunkapiller, M. W., Hewick, R. M., Dreyer, W. J., and Hood, L. E. (1983) *Methods Enzymol.* **91,** 399–413
31. Engel, J., Odermatt, E., Engel, A., Madri, J. A., Furthmayr, H., Rohde, H., and Timpl, R. (1981) *J. Mol. Biol.* **150,** 97–120
32. Ruano, M. L., Perez-Gil, J., and Casals, C. (1998) *J. Biol. Chem.* **273,** 15183–15191
33. Ruano, M. L., Miguel, E., Perez-Gil, J., and Casals, C. (1996) *Biochem. J.* **313,** 683–689
34. Skelly, R. R., Munkenbeck, P., and Morrison, D. C. (1979) *Infect. Immun.* **23,** 287–293
35. Canadas, O., Guerrero, R., García-Cañero, R., Orellana, G., Menéndez, M., and Casals, C. (2004) *Biochemistry* **43,** 9926–9938
36. Ruano, M. L., Garcia-Verdugo, I., Miguel, E., Perez-Gil, J., and Casals, C. (2000) *Biochemistry* **39,** 6529–6537
37. Casals, C., Herrera, L., Miguel, E., Garcia-Barreno, P., and Municio, A. M. (1989) *Biochim. Biophys. Acta* **1003,** 201–203
38. Wenstrup, R. J., Shrago-Howe, A. W., Lever, L. W., Phillips, C. L., Byers, P. H., and Cohn, D. H. (1991) *J. Biol. Chem.* **266,** 2590–2594
39. Haagsman H. P., Sargeant, T., Hauschka, P. V., Benson, B. J., and Hawgood, S. (1990) *Biochemistry* **29,** 8894–8900
40. Tobias, P. S., Soldau, K., Iovine, N. M., Elsbach, P., and Weiss, J. (1997) *J. Biol. Chem.* **272,** 18682–18685

41. Viriyakosol, S., Mathison, J. C., Tobias, P. S., and Kirkland, T. N. (2000) *J. Biol. Chem.* **275,** 3144–3149
42. da Silva Correia, J., Soldau, K., Christen, U., Tobias, P. S., and Ulevitch, R. J. (2001) *J. Biol. Chem.* **276,** 21129–21135
43. Takayama, K., Mitchell, D. H., Din, Z. Z., Mukerjee, P., Li, C., and Coleman, D. L. (1994) *J. Biol. Chem.* **269,** 2241–2244
44. Van Iwaarden, J. F., Pikaar, J. C., Storm, J., Brouwer, E., Verhoef, J., Oosting, R. S., van Golde, L. M., and van Strijp, J. A. (1994) *Biochem. J.* **303,** 407–411
45. Stamme, C., Muller, M., Hamann, L., Gutsmann, T., and Seydel, U. (2002) *Am. J. Respir. Cell Mol. Biol.* **27,** 353–360
46. Wallis, R., and Drickamer, K. (1999) *J. Biol. Chem.* **274,** 3580–3589
47. McCormack, F. X., Damodarasamy, M., and Elhalwagi, B. M. (1999) *J. Biol. Chem.* **274,** 3173–3181
48. Palaniyar, N., Zhang, L., Kuzmenko, A., Ikegami, M., Wan, S., Wu, H., Korfhagen, T. R., Whitsett, J. A., and McCormack, F. X. (2002) *J. Biol. Chem.* **277,** 26971–26979
49. Ridsdale, R. A., Palaniyar, N., Holterman, C. E., Inchley, K., Possmayer, F., and Harauz, G. (1999) *Biochim. Biophys. Acta* **1453,** 23–34
50. Palaniyar, N., Ridsdale, R. A., Possmayer, F., and Harauz, G. (1998) *Biochem. Biophys. Res. Commun.* **250,** 131–136
51. Worthman, L. A., Nag, K., Rich, N., Ruano, M. L., Casals, C., Perez-Gil, J., and Keough, K. M. (2000) *Biophys. J.* **79**, 2657–2666
52. Ikegami, M., Elhalwagi, B. M., Palaniyar, N., Dienger, K., Korfhagen, T. R., Whitsett, J. A., and McCormack, F. X. (2001) *J. Biol. Chem.* **276,** 38542–38548
53. Palaniyar, N., McCormack, F. X., Possmayer, F., and Harauz, G. (2000) *Biochemistry* **39,** 6310–6316
54. Kitchens, R. L., and Munford, R. S. (1998) *J. Immunol.* **160,** 1920–1928
55. Sano, H., Chiba, H., Iwaki, D., Sohma, H., Voelker, D. R., and Kuroki, Y. (2000) *J. Biol. Chem.* **275,** 22442–22451